0026-895X/02/6202-406–414$7.00
MOLECULAR PHARMACOLOGY
Vol. 62, No. 2
1591/997653
Mol Pharmacol 62:406–414, 2002
Printed in U.S.A.

Nicotinic Receptor M3 Transmembrane Domain: Position 8′ Contributes to Channel Gating

MARÍA JOSÉ DE ROSA, DIEGO RAYES, GUILLERMO SPITZMAUL, and CECILIA BOUZAT

Instituto de Investigaciones Bioquímicas, Universidad Nacíonal del Sur-Consejo Nacional de Investigaciones Científicas y Técnicas, Bahía Blanca, Argentina

Received January 7, 2002; accepted April 30, 2002

This article is available online at http://molpharm.aspetjournals.org

ABSTRACT

The nicotinic acetylcholine receptor (nAChR) is a pentamer of homologous subunits with composition $\alpha_2\beta\epsilon\delta$ in adult muscle. Each subunit contains four transmembrane domains (M1–M4). Position 8′ of the M3 domain is phenylalanine in all heteromeric α subunits, whereas it is a hydrophobic nonaromatic residue in non-α subunits. Given this peculiar conservation pattern, we studied its contribution to muscle nAChR activation by combining mutagenesis with single-channel kinetic analysis. Construction of nAChRs carrying different numbers of phenylalanine residues at 8′ reveals that the mean open time decreases as a function of the number of phenylalanine residues. Thus, all subunits contribute through this position independently and additively to the channel closing rate. The impairment of channel opening increases when the number of phenylalanine residues at 8′ increases from two (wild-type nAChR) to five. The gating equilibrium constant of the latter mutant nAChR is 13-fold lower than that of the wild-type nAChR. The replacement of αF8′, βL8′, δL8′, and ϵV8′ by a series of hydrophobic amino acids reveals that the structural bases of the observed kinetic effects are nonequivalent among subunits. In the α subunit, hydrophobic amino acids at 8′ lead to prolonged channel lifetimes, whereas they lead either to normal kinetics (δ and ϵ subunits) or impaired channel gating (β subunit) in the non-α subunits. The overall results indicate that 8′ positions of the M3 domains of all subunits contribute to channel gating.

The nicotinic acetylcholine receptor (nAChR) is a pentamer of homologous subunits. The primordial nAChR pentamer presumably contained only one type of α subunit, exemplified by the α7 homopentamer found in the brain. However, evolution led to subunit diversity, resulting in a wide spectrum of structurally and functionally different nAChRs (Le Novere and Changeux, 1995). nAChRs at the motor synapse are heteropentamers with a subunit composition of $\alpha_2\beta\epsilon\delta$ in adult muscle. All α subunits are characterized by the presence of a pair of adjacent cysteines in the N-terminal domain. Non-α subunits (lacking the pair of cysteines) have derived from α subunits (Ortells and Lunt, 1995). Sequence comparison of subunits reveals several candidate residues in transmembrane domains differentially conserved between the two types of subunits (heteromeric α and non-α subunits). In addition, many of these residues are also conserved between non-α subunits and homomeric α subunits. This peculiar pattern of conservation led us to believe it could represent structures important for proper function. We therefore examined contributions to channel activation of residues in the M3 transmembrane domain of the heteromeric muscle nAChR, which are conserved among homomeric α and non-α subunits but differ in the heteromeric α subunits.

Each nAChR subunit contains an amino-terminal extracellular domain of approximately 210 amino acids, four transmembrane domains (M1-M4) and a short extracellular carboxy-terminal tail. The M2 domain of each subunit contributes to the cation-selective channel, and agonist binding triggers its twisting to allow ion flow (Unwin, 1995). The locations, secondary structures, and functional roles of the M1, M3, and M4 transmembrane domains are not as well understood. The pattern of incorporation of the hydrophobic probe 3-trifluoromethyl-3-*m*-[^{125}I]-iodophenyldiazirine (TID) in *Torpedo californica* nAChR (Blanton and Cohen, 1994), NMR (Lugovskoy et al., 1998) and Fourier transform infrared spectroscopy studies (Baenziger and Methot, 1995; Methot et al., 2001) support a transmembrane organization of M3 in an α-helix with some contact with the lipid bilayer, whereas cryoelectron microscopic studies suggest β-sheet structures for M1, M3, and M4 (Unwin, 1993). A few lines of experimental evidence indicate that M3 is a key component of the nAChR channel gating apparatus: 1) by using α7/α3

This work was supported by grants from Ministerio de Salud de la Nación, Universidad Nacional del Sur, Agencia Nacional de Promoción Científica y Tecnológica Third World Academy of Sciences (to C.B.); and Fogarty International Research Collaboration grant 1R03-TW01185-01 [to Dr. Steven M. Sine (Mayo Foundation, Rochester, MN) and C.B.].

M.J.D.R and D.R. contributed equally to this work.

ABBREVIATIONS: nAChR, nicotinic acetylcholine receptor; ACh, acetylcholine; M3, third transmembrane domain; HEK, human embryonic kidney; P_{open}, channel open probability.

chimeric subunits, Campos-Caro et al. (1997) demonstrated that the M3 domain influences the gating of neuronal nAChRs; 2) a mutation at position 9′ of M3 of the α subunit has been found in a patient suffering from a congenital myasthenic syndrome (Wang et al., 1999). Kinetic analysis of engineered mutant nAChRs revealed that this position is essential for the opening and closing of the nAChR (Wang et al., 1999); and 3) tryptophan substitutions at lipid-exposed residues of the γ M3 transmembrane domain of *T. californica* nAChR increased the macroscopic currents of the resulting nAChRs (Cruz-Martin et al., 2001).

Position 8′ of the M3 domain is phenylalanine in all heteromeric α subunits but is a hydrophobic nonaromatic residue in homomer-forming α subunits and non-α subunits. Given this particular conservation pattern, we study its contribution to channel gating by combining site-directed mutagenesis and single-channel recordings. Our studies reveal that all subunits contribute independently and additively to the closing step through this position. In addition, the concentration-dependence of receptor activation is shifted toward higher agonist concentrations as a function of the number of phenylalanine residues at position 8′ of M3.

Materials and Methods

Construction of Mutant Subunits. Mouse cDNAs were subcloned into the cytomegalovirus-based expression vector pRBG4 (Sine, 1993). Mutant subunits were constructed using the QuikChange site-directed mutagenesis kit (Strategene, Inc., La Jolla, CA). Restriction mapping and DNA sequencing confirmed all constructs.

Expression of nAChR. HEK293 cells were transfected with α, β, δ, and ϵ cDNA subunits (wild-type or mutants) using calcium phosphate precipitation at a subunit ratio of 2:1:1:1 for $\alpha/\beta/\delta/\epsilon$, respectively, essentially as described previously (Bouzat et al., 1994, 1998). All α subunits contained a valine at position 433 of M4 according to the GenBank database (Salamone et al., 1999). For transfections, cells at 40 to 50% confluence were incubated for 8 to 12 h at 37°C with the calcium phosphate precipitate containing the cDNAs in DMEM plus 10% fetal bovine serum. Cells were used for single-channel measurements 1 or 2 days after transfection.

Patch-Clamp Recordings. Recordings were obtained in the cell-attached configuration (Hamill et al., 1981) at a membrane potential of −70 mV and at 20°C. The bath and pipette solutions contained 142 mM KCl, 5.4 mM NaCl, 1.8 mM $CaCl_2$, 1.7 mM $MgCl_2$ and 10 mM HEPES, pH 7.4. Patch pipettes were pulled from 7052 capillary tubes (Garner Glass, Claremont, CA) and coated with Sylgard (Dow Corning, Midland, MI). Pipette resistance ranged from 5 to 7 MΩ. Acetylcholine (ACh) at final concentrations of 1 to 1000 μM or choline at 100 μM or 20 mM was added to the pipette solution.

Single-channel currents were recorded using an Axopatch 200 B patch-clamp amplifier (Axon Instruments, Inc., Union City, CA), digitized at 5-μs intervals with the PCI-6111E interface (National Instruments, Austin, TX), recorded to the hard disk of a computer using the program Acquire (Bruxton Corporation, Seattle, WA), and detected by the half-amplitude threshold criterion using the program TAC 4.0.10 (Bruxton Corporation) at a final bandwidth of 10 kHz. Data of nAChRs activated by 20 mM choline were recorded at a membrane potential of −70 mV and analyzed at a bandwidth of 5 kHz to avoid detection of some blockages that could be resolved at 10 kHz. In this manner, channel kinetics can be reduced to those of the closed-to-open reaction (Grosman and Auerbach, 2000; Bouzat et al., 2002).

Open- and closed-time histograms were plotted using a logarithmic abscissa and a square root ordinate (Sigworth and Sine, 1987) and fitted to the sum of exponential functions by maximum likelihood using the program TACFit (Bruxton Corporation). Open probability within clusters (P_{open}) was determined experimentally at each ACh concentration by calculating the mean fraction of time that the channel is open within a cluster.

Kinetic Analysis. Kinetic analysis was performed as described previously (Wang et al., 1997; Bouzat et al., 2000, 2002). The analysis was restricted to clusters of channel openings, each reflecting the activity of a single nAChR. Clusters of openings corresponding to a single channel were identified as a series of closely spaced events preceded and followed by closed intervals longer than a critical duration (τ_{crit}). This duration was taken as the point of intersection of the predominant closed component and the succeeding one in the closed-time histogram. The predominant closed duration component became shorter with the increase of agonist concentration. Consequently, we assume that this component reflects the set of transitions between unliganded closed and diliganded open states. To minimize errors in assigning cluster boundaries, we analyzed only recordings from patches with low channel activity in which both components are clearly differentiated from one another. Because each cluster contains one more opening than closing, to avoid biasing in favor of openings, only clusters containing more than 10 openings were considered for further analysis. In addition, clusters showing double openings were rejected.

For each recording, kinetic homogeneity was determined by selecting clusters on the basis of their distribution of mean open duration, mean closed duration, and open probability (Wang et al., 1997; Bouzat et al., 2000, 2002). Typically, the distributions contained an approximately Gaussian dominant component and minor contributions of clusters with different properties. Clusters showing open time, closed time, and open probability values within 2 S.D. of the mean of the major component were selected. Typically, more than 80% of the clusters were selected and only the non-Gaussian appendages were omitted (Bouzat et al., 2002). Mean values obtained from distributions of open probability, mean open channel duration, and mean closed channel duration of clusters do not change significantly after the selection procedure (Bouzat et al., 2002). In addition, comparison of closed- and open-time histograms before and after selection indicates that the selected clusters are representative of the predominant population of nAChR in the patch (Bouzat et al., 2000).

The resulting open and closed intervals from single patches at several ACh concentrations were analyzed according to kinetic schemes using the program MIL (QuB suite, State University of New York, Buffalo). Briefly, the program allows simultaneous fitting of recordings at different agonist concentrations and estimates the rate constants using a maximum likelihood method that corrects for missed events (Qin et al., 1996). The dead time was typically 30 μs. Probability density functions of open and closed durations were calculated from the fitted rate constants and instrumentation dead time and superimposed on the experimental dwell-time histogram as described by Qin et al. (1996). Calculated rates were accepted only if the resulting probability density functions correctly fit the experimental open- and closed-duration histograms.

For wild-type and some mutant nAChRs activated by Ach, the opening rate of the diliganded nAChR, β_2 in Scheme 1, was constrained to its previously determined value (Sine et al., 1995; Wang et al., 1997; Salamone et al., 1999) because brief closings caused by gating and channel blocking become indistinguishable at high ACh concentrations (Wang et al., 1997; Salamone et al., 1999; Bouzat et al., 2000). When β_2 was allowed to vary freely, MIL failed to converge to a well-defined set of rate constants and approached a value of about 100,000/s (Salamone et al., 1999; Bouzat et al., 2000). Also, association and dissociation rate constants were assumed to be equal at both binding sites (Akk and Auerbach, 1996; Wang et al., 1997; Salamone et al., 1999). Rate constants are shown with S.D.

Results

Additivity of the Effects of Mutations at Position 8′ of M3. Position 8′ of the M3 domain is phenylalanine (F) in all heteromeric α subunits but is a hydrophobic nonaromatic residue in homomer-forming α subunits and non-α subunits (Fig. 1). Replacement of F8′ in α1 by its homologous in the α7 subunit, isoleucine, increases the mean open time of the resulting nAChRs (Fig. 2). On the contrary, the reverse mutations at β, δ and ϵ subunits decrease the mean open time. At 1 μM ACh, open-time distributions of wild-type nAChRs show a major component of about 900 μs with a relative amplitude larger than 0.8 in all recordings (Table 1). nAChRs containing the mutant αF8′I subunits form channels characterized by increased mean open times whereas open durations of nAChR channels containing the mutant βL8′F, ϵV8′F, or δL8′F subunits are significantly briefer than those of wild-type (Table 1).

The increase in the mean open time in the αF8′ I nAChR is also observed when channels are activated by choline instead of acetylcholine. Mean open times of channels recorded in the presence of 100 μM choline were 190 ± 10 μs and 540 ± 30 μs for wild-type and αF8′ I nAChRs, respectively.

Given that the introduction of phenylalanine residues to 8′ of non-α subunits decreases the measured duration of apparent openings and the removal of phenylalanine from the α subunit produces the opposite effect, we investigated the relationship between the number of F residues at 8′ and the channel mean open time. We combined wild-type and mutant subunits to construct single nAChRs containing a variable number of F residues, ranging from 0 (αF8′I) to 5. As shown in Fig. 3, the mean open time decreases systematically with the increase in the number of F residues at 8′.

Figure 4 shows that the duration of the open state depends on the number of F residues. Each phenylalanine makes additive contributions to the energy barrier of the closing process, reducing it by ~0.5 kcal/mol. In all cases, nAChR channels carrying the mutant β subunit seem to be slightly briefer, indicating a not very significant asymmetry in the contribution of the different subunits to the duration of the open state (Fig. 4 and Table 1).

At concentrations higher than 10 μM, wild-type as well as all mutant nAChRs open in clusters of well defined activation episodes. Each cluster reflects the activity of a single nAChR (Sakmann et al., 1980). For both wild-type and mutant nAChRs, histograms of closed intervals show a predominant component that becomes progressively briefer with increasing ACh concentration. This component reflects the set of transitions between unliganded closed and diliganded open states. Table 2 shows the mean durations of the predominant closed component for wild-type and mutant nAChRs activated by 30 μM ACh. As shown in Table 2, this time increases with the number of phenylalanine residues present at position 8′. Statistically, the duration of this component is significantly longer in the F = 5 nAChR than in the control (F = 2) ($p < 0.005$, Student's t test). Prolonged closed times could be caused by changes in rate constants underlying either ACh binding or channel gating steps.

Kinetic Changes Caused by the Presence of Phenylalanine Residues at Position 8′ of M3. To identify unequivocally the kinetic steps affected by the presence of phenylalanine residues at position 8′, and to quantify the kinetic

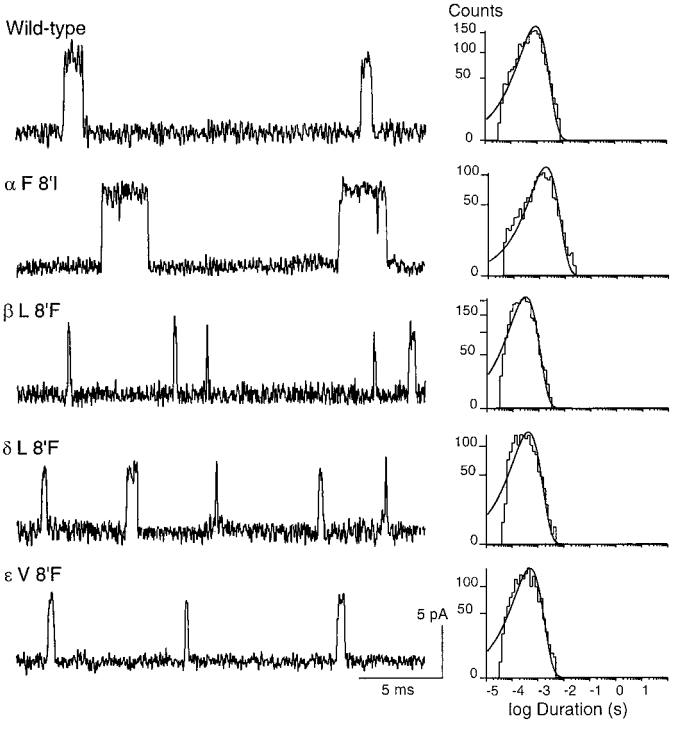

Fig. 2. Effect of mutations at position 8′ of M3. Right, channels activated by 1 μM ACh were recorded from HEK cells expressing nAChRs containing wild-type and the mutant subunits αF8′I, βL8′F, ϵV8′F or δL8′F. Currents are displayed at a bandwidth of 9 kHz with channel openings as upward deflections. Membrane potential: −70 mV. Left, open-time histograms of nAChRs carrying the specified mutant subunit.

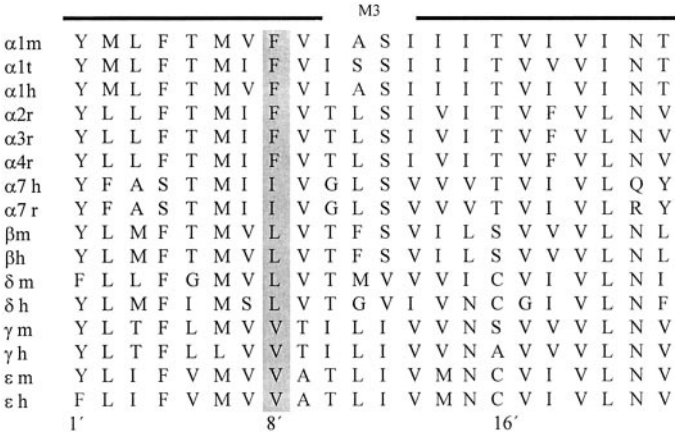

Fig. 1. Sequence alignment of the M3 transmembrane domain of different subunits.

TABLE 1

Open durations of mutant AChRs

Recordings were obtained from cells expressing AChRs containing the indicated mutant subunit and activated by 1 μM ACh. The mean open times were obtained from the corresponding open-time histograms. n is the number of recordings for each condition.

Mutant Subunit	Mean Open Time	n
	ms	
Wild-type	0.90 ± 0.14	6
αF8′I	1.75 ± 0.30	8
βL8′F	0.30 ± 0.05	5
δL8′F	0.40 ± 0.07	8
εV8′F	0.45 ± 0.14	6

changes, we fitted kinetic schemes to the open- and closed-dwell time histograms of mutant nAChRs.

nAChR channels were activated by a range of desensitizing concentrations of ACh (10 to 300 μM) to produce clear clusters of events corresponding to a single channel (Sakmann et al., 1980). Because each cluster of channel openings reflects the activity of a single nAChR, closed and open times of the selected clusters were used for the kinetic analysis.

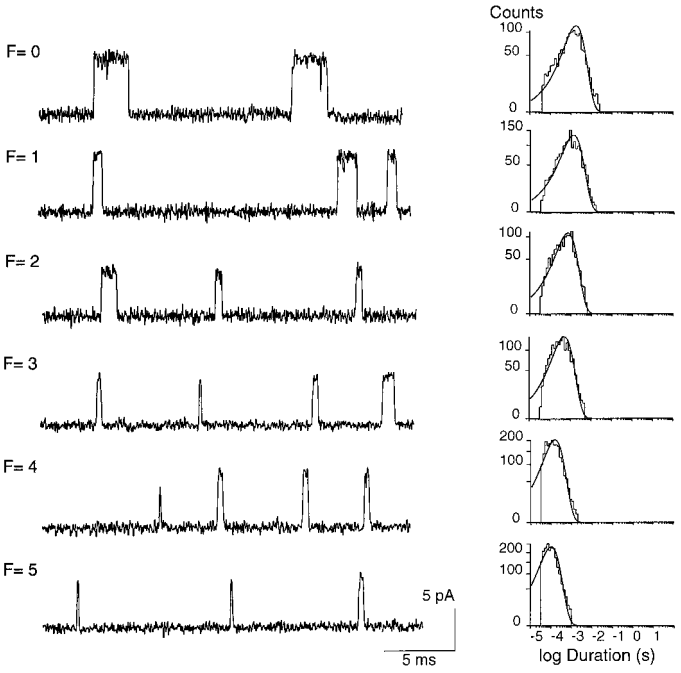

Fig. 3. nAChRs containing different numbers of F residues at 8′ M3. Right, channels activated by 1 μM ACh expressing different numbers of wild-type and mutant (m) subunits at 8′ of M3 to yield nAChRs containing a number of F residues ranging from 0 (F = 0) to 5 (F = 5). The recordings correspond to: F = 0, $\alpha_m\beta\epsilon\delta$; F = 1, $\alpha_m\beta\epsilon_m\delta$; F = 2, wild-type; F = 3, $\alpha\beta\epsilon\delta_m$; F = 4, $\alpha\beta_m\epsilon\delta_m$; and F = 5, $\alpha\beta_m\epsilon_m\delta_m$. Mutant subunits are: αF8′I, βL8′F, ϵV8′F, and δL8′F. Currents are displayed at a bandwidth of 9 kHz with channel openings as upward deflections. Membrane potential: −70 mV. Left, open-time histograms of nAChRs carrying the specified mutant subunit.

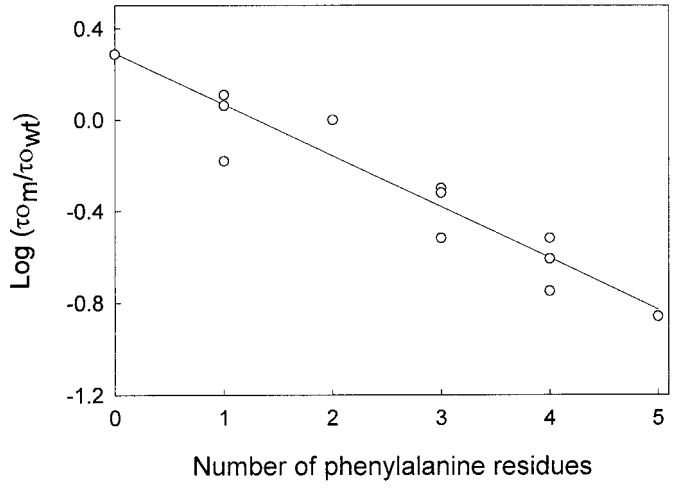

Fig. 4. Ratio of mean open time of mutant nAChRs with respect to that of wild-type nAChR as a function of the number of phenylalanine residues at position 8′ of M3. Mean open times (τo) were obtained from the corresponding open-time histograms of at least four recordings for each condition. Ratios plotted on a log scale display the data on a linear free energy scale. The symbols correspond to the following nAChRs: F = 0, $\alpha_m\beta_{wt}\epsilon_{wt}\delta_{wt}$; F = 1, $\alpha_m\beta_{wt}\epsilon_m\delta_{wt}$, $\alpha_m\beta_{wt}\epsilon_{wt}\delta_m$, and $\alpha_m\beta_m\epsilon_{wt}\delta_{wt}$; F = 2, wild-type; F = 3, $\alpha_{wt}\beta_{wt}\epsilon_m\delta_{wt}$, $\alpha_{wt}\beta_{wt}\epsilon_{wt}\delta_m$, and $\alpha_{wt}\beta_m\epsilon_{wt}\delta_{wt}$; F = 4, $\alpha_{wt}\beta_{wt}\epsilon_m\delta_m$, $\alpha_{wt}\beta_m\epsilon_m\delta_{wt}$, and $\alpha_{wt}\beta_m\epsilon_{wt}\delta_m$; F = 5, $\alpha_{wt}\beta_m\epsilon_m\delta_m$. Mutant subunits are: αF8′I, βL8′F, ϵV8′F, and δL8′F.

For wild-type nAChRs, we used the classical activation scheme shown in Scheme 1, where two agonists (A) bind to the receptor (R) in the resting state with association rates k_{+1} and k_{+2}, and dissociate with rates k_{-1} and k_{-2}. Receptors occupied by one agonist open with rate β_1 and close with rate α_1, and nAChRs occupied by two agonist molecules open with rate β_2 and close with rate α_2. At high agonist concentrations (higher than 100 μM ACh), channel blockade is evident; thus, the blocked state, A_2B, is included in the scheme. Omitting blockade from Scheme 1 does not affect significantly the calculated rate constants (Salamone et al., 1999; data not shown). Because some of the blockages at 300 μM ACh are resolved under the present conditions, the incorporation of the channel blockade to the model improves the fitting of the histograms corresponding to high agonist concentrations (data not shown).

To estimate the set of rate constants, Scheme 1 was fitted to the data using the program MIL (Qin et al., 1996). We simultaneously analyzed recordings obtained at multiple ACh concentrations (10–300 μM) with the aim of representing all the states in Scheme 1 in the analysis. Rate constant estimates obtained for wild-type nAChR (F = 2 in Table 3) agree with those previously reported for mouse nAChR (Akk and Auerbach, 1996; Wang et al., 1997; Salamone et al., 1999; Bouzat et al., 2000).

Compared with wild-type, the F = 5 mutant nAChRs show both briefer openings and prolonged intracluster closings at all ACh concentrations (Fig. 5). The smooth curves through the open and closed dwell time histograms show that Scheme 1 adequately describes activation of F = 5 mutant receptors (Fig. 5). The resulting analysis establishes that the closing rate markedly increases and the opening rate decreases in mutant nAChRs containing five F residues at 8′ of M3 (Table 3).

The kinetic analysis applied to mutant nAChRs containing different numbers of F residues indicates that position 8′ governs mainly the opening and closing steps (Table 3). As shown in this table, increasing the number of F residues makes the nAChR open with greater latency and close more rapidly.

Kinetic analysis of nAChRs containing the mutant αF8′I subunit, lacking F residues at 8′ (F = 0), shows that the

TABLE 2

Mean closed times of mutant nAChRs activated by 30 μM ACh

Recordings were obtained from HEK cells transfected with wild-type and mutant subunits to yield nAChRs containing different number of phenylalanine residues at 8′, ranging from 0 (F = 0) to 5 (F = 5). The mean closed time corresponds to the predominant component of the closed-time histogram which is associated to closings within clusters. n is the number of recordings for each condition.

Number of F Residues	Mutant Subunits	Mean Closed Time	*n*
		ms	
0	αF8′I	1.80 ± 0.60	4
1	αF8′I, δL8′F	2.30 ± 0.25	3
2	Wild-type	1.30 ± 0.18	6
3	ϵV8′F	2.40 ± 0.14	4
4	ϵV8′F, δL8′F	2.70 ± 0.20	5
4	βL8′F, δL8′F	5.60 ± 1.70	4
5	βL8′F, ϵV8′F, δL8′F	5.00 ± 1.20	5

closing rate decreases in this mutant nAChR (Table 3). This result agrees with the observation that in this mutant nAChR the duration of the open state increases. As described above for wild-type, β_2 had to be constrained to its known value to allow the fitting. As a consequence, if the opening rate changed, it was not possible to detect it. In this respect, when the fixed value of β_2 was systematically reduced from 50,000 s^{-1} to 30,000 s^{-1}, the best description based on likelihood was obtained with the highest value of β_2. The fit using β_2 = 50,000 s^{-1} was e^2, e^5, and e^{15} times more likely than with β_2 equal to 45,000, 40,000, and 30,000 s^{-1}, respectively.

To determine whether the rate of channel opening increased in nAChRs lacking F residues at 8′, we used saturating concentrations of choline, an agonist with a very slow opening rate (Grosman and Auerbach, 2000). Recordings of αF8′I nAChRs activated by 20 mM choline appear, as for wild-type, in clusters of channel events showing a 50% reduction in channel amplitude due to open-channel block (2.8 ± 0.3 pA instead of about 5.5 pA for channels activated by ACh or choline at concentrations lower than 100 μM at −70 mV (see Grosman and Auerbach, 2000; Bouzat et al.,

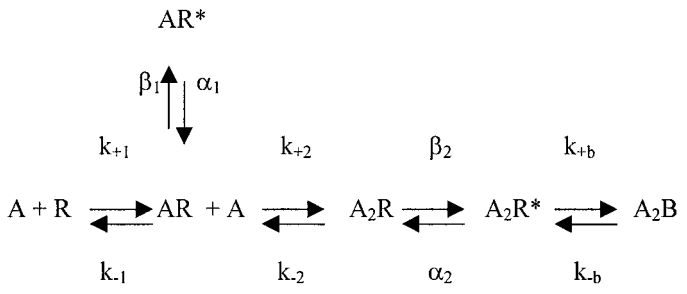

Scheme 1.

TABLE 3

Kinetic parameters for mouse wild-type and M3 mutant AChRs

The data correspond to AChRs containing 0 (F = 0) to 5 (F = 5) F residues at 8′. Rate constants are in units of $\mu M^{-1}\ s^{-1}$ for association rate constants and s^{-1} for all others. Values are results of a global fit of Scheme 1 to data obtained over a range of concentration of ACh. Standard errors are shown. Data not showing standard errors have been constrained to allow a better fit. The mutant nAChRs are: F = 0, $\alpha_m\beta_{wt}\varepsilon_{wt}\delta_{wt}$; F = 2, wild-type; F = 3, $\alpha_{wt}\beta_{wt}\varepsilon_m\delta_{wt}$; F = 4, (ε, δ) $\alpha_{wt}\beta_{wt}\varepsilon_m\delta_m$; (β, ε) $\alpha_{wt}\beta_m\varepsilon_m\delta_{wt}$; and F = 5, $\alpha_{wt}\beta_m\varepsilon_m\delta_m$. Mutant subunits are: αF8′I, βL8′F, εV8′F and δL8′F.

No. of F (Mutant subunits)	k_{+1}	k_{-1}	k_{+2}	k_{-2}	β_1	α_1	β_2	α_2	k_{+b}	k_{-b}
F = 0	100	22,000	50	44,000	960	1,200	50,000	660	4	78,000
(α)	±4	±1,300	±2	±2,700	±60	±60		±25	±2	
WT	330	28,000	170	56,000	640	2,600	50,000	1,500	9	78,000
F = 2	±40	±2,500	±20	±5,000	±40	±140		±100	±1	±6,000
F = 3	340	32,000	170	64,000	170	7,600	28,000	3,500	2	78,000
(ε)	±15	±1,000	±10	±2,100	±10	±800	±1,900	±130	±1	
F = 4	340	32,600	170	65,000	100	8,000	26,000	2,600	15	78,000
(ε, δ)	±30	±1,300	±20	±2,700	±10	±1,000	±1,100	±200	±5	
F = 4	400	40,000	200	85,000	N.D.	N.D.	25,000	3,600	10	78,000
(β, ε)	±4	±4,300	±2	±9,700			±1,500	±100	±2	
F = 5	290	25,000	145	51,000	400	11,900	14,800	6,100	8	78,000
(β, ε, δ)	±13	±1,000	±7	±2,000	±30	±700	±600	±100	±1	

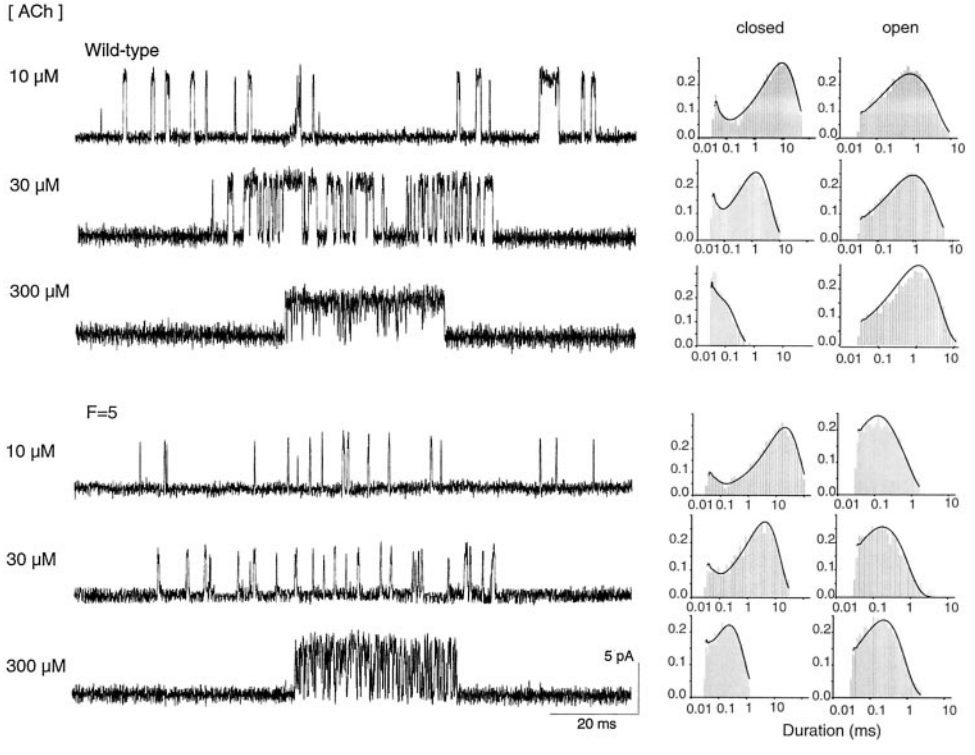

Fig. 5. Kinetics of activation of wild-type and mutant nAChRs. Left, channel traces corresponding to nAChRs containing two (wild-type) or five (F = 5) phenylalanine residues at position 8′ of M3 and activated by 10, 30, and 300 μM ACh. Currents are displayed at a bandwidth of 9 kHz with channel openings as upward deflections. Center and right, closed- and open-time histograms corresponding to the selected clusters with the fit for scheme 1 superimposed. The ordinates correspond to the square root of the fraction of events per bin. F = 5 nAChR is composed of the following subunits: α, βL8′F, εV8′F, and δL8′F.

2002; Fig. 6). For both wild-type and mutant choline-activated nAChRs, open-time histograms are well described by a single component and closed-time histograms show a main component that corresponds to closings within clusters (Fig. 6). Given that 20 mM choline is a saturating agonist concentration (Grosman and Auerbach, 2000), we fitted dwell times from the selected clusters to a kinetic scheme containing only one open and one closed state. Under these conditions, the estimates for opening and closing rate constants are: wild-type: $90 \pm 20\ s^{-1}$ and $1732 \pm 214\ s^{-1}$ for β and α, respectively (mean $\pm$ S.D. of seven different patches); αF8′I, $60 \pm 20\ s^{-1}$ and $893 \pm 230\ s^{-1}$ for β and α, respectively (mean $\pm$ S.D. of four different recordings). Thus, the resulting rate constant estimates indicate that αF8′I does not affect significantly the rate of channel opening ($p > 0.1$, Student's t test) and confirm the decrease in the rate of channel closing ($p < 0.01$).

Given that under our experimental conditions the currents of both wild-type and αF8′ I nAChRs decrease about 50% in the presence of 20 mM choline, we estimate K_B (k_{-b}/k_{+b}) to be approximately 20 mM for both nAChRs in agreement with Grosman and Auerbach (2000). Considering the classical blocking scheme (C $\leftrightarrow$ O $\leftrightarrow$ OB), the mean duration of apparent openings at 20 mM choline would be two-fold longer than that in the absence of blockade (Grosman and Auerbach, 2000). Accordingly, the mean duration of apparent openings of channels activated by 20 mM choline are approximately two-fold longer than that of channels activated by 100 μM choline for both wild-type and αF8′ I nAChRs. Therefore, the closing rate-constant estimates for choline may be underestimated by a factor of $\sim$2 as reported previously (Grosman and Auerbach, 2000).

Changes in Free Energy. The channel gating equilibrium constant for ACh-activated receptors, θ, calculated as β_2/α_2, decreases as a function of the number of F residues at position 8′ of M3. This constant decreases from 33 in the wild-type nAChR (F = 2) to 2.4 in the F = 5 mutant nAChR. This decrease corresponds to a free energy change of 1.5 kcal/mol. nAChRs containing an intermediate number of F residues between two and five show intermediate values of θ. Calculated values of θ for nAChRs containing three and four F residues are: 8 for F = 3 (mutant ϵ subunit); 10 and 6.9 for F = 4 (mutant ϵ and δ subunits and mutant β and ϵ subunits, respectively). In contrast, θ increases approximately two-fold in the F = 0 mutant nAChR containing the αF8′I mutant subunit (θ = 75).

Probability of Channel Opening in 8′ M3 Mutants. To determine the overall consequences for receptor activation of mutations at 8′, we determined the open probability as a function of ACh concentration. For wild-type nAChRs, the open probability increases with increasing ACh concentration, showing an EC_{50} of about 40 μM. The curve shifts progressively to the right as the number of F residues increases. The profile for the F = 5 mutant nAChR shift to higher ACh concentrations, increasing the EC_{50} to 110 μM and lowering the maximum P_{open} to approximately 0.6 at 1 mM ACh (Fig. 7). The EC_{50} and maximum open probability values for mutant nAChRs are 57 μM and 0.88 for F = 3 (mutant ϵ subunit), 100 μM and 1.0 for F = 4 (mutant ϵ and δ subunits), and 100 μM and 0.92 for F = 4 (mutant ϵ and β subunits). On the contrary, the profile for nAChRs lacking F residues at 8′ (F = 0) is slightly displaced to the left (EC_{50} = 32 μM and maximum P_{open} 0.98).

Structural Bases of Kinetic Effects of Mutations at Position 8′ of M3. Because the mutations βL8′F, δL8′F, and ϵV8′F impair channel gating and the αF8′I produces the opposite effect, we further investigated whether these kinetic changes are specific to these mutations or if they respond to a more general hydrophobic nonaromatic versus aromatic change. We engineered a series of hydrophobic side chains at 8′, recorded single-channel currents elicited by 30 μM ACh, and analyzed the kinetic properties of the nAChR clusters. We chose a concentration of 30 μM because it is close to the EC_{50} for the adult muscle nAChR and therefore it is sensitive to changes in activation parameters. For each cluster within a recording, we calculated the P_{open}, mean open duration, and mean closed duration; plotted their distributions; and determined the mean values. Figure 8 shows the mean values of these parameters for the different mutant subunits.

In the α subunit, substitution of F8′ by the hydrophobic amino acids alanine, leucine, and valine increases the mean open duration by about 2- (αF8′A and αF8′L) and 2.5-fold (αF8′V). Thus, hydrophobic amino acids similarly increase

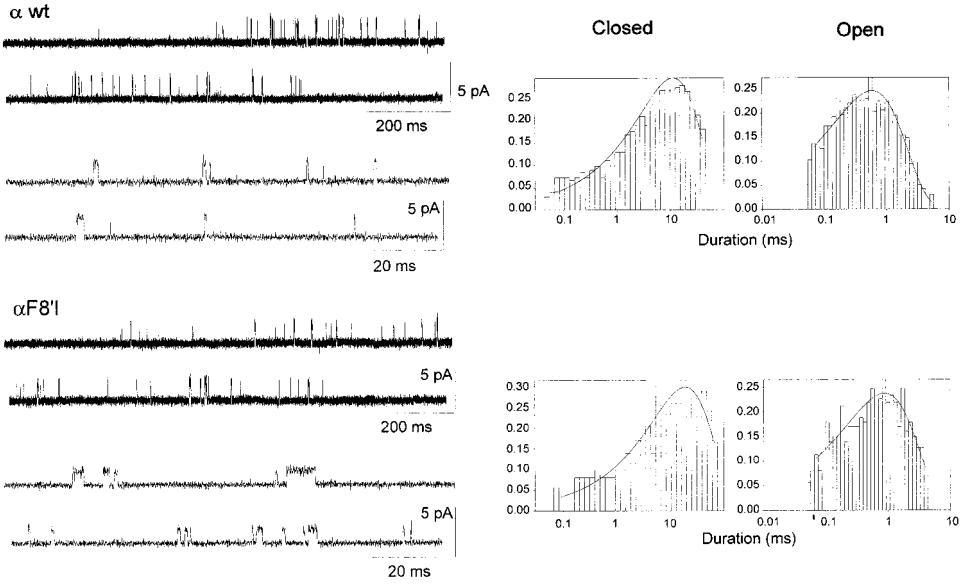

Fig. 6. Single-channel currents in the presence of 20 mM choline. Left, channel traces corresponding to nAChRs containing α wild-type or αF8′I subunits. Continuous recordings are shown in two traces for each time scale. Membrane potential, −70 mV. Openings are shown as upward deflections at a bandwidth of 5 kHz. Right, open and closed time histograms with the fit superimposed to the experimental histograms. Histograms were constructed with the selected clusters and the ordinates correspond to the square root of the fraction of events per bin.

the duration of the open state. nAChRs containing the αF8′L subunit are almost identical to those containing αF8′I (Fig. 8), indicating that channel gating is not influenced by the stereochemistry of the side chain. The mutations αF8′A and αF8′V produce, in addition to the increased open time, an increase in the duration of the closed component associated to the set of transitions between unliganded closed and diliganded open states, such increase leading to a slight decrease in the P_{open} with respect to that observed with L and I (Fig. 8). There seems not to be a straightforward explanation for the increase in the closed time. In terms of hydrophobicity, alanine is less hydrophobic than isoleucine whereas valine is similar to isoleucine (Kyte and Doolittle, 1982) and the helical propensity in a nonpolar environment of valine is very similar to that of leucine (Liu and Deber, 1998). Alanine and valine have smaller volumes than isoleucine and leucine. However, although valine has an intermediate size between alanine and leucine, it produces a more significant increase in the duration of the closed time than alanine does.

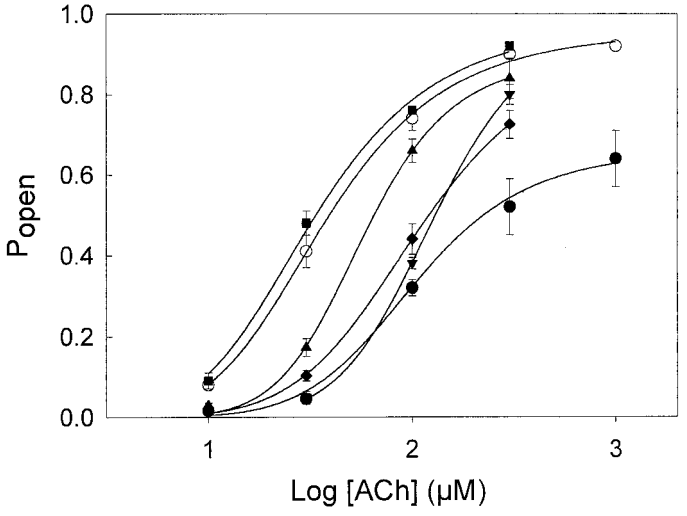

Fig. 7. Agonist concentration dependence of the channel open probability. The mean fraction of time the channel is open during a cluster (P_{open}) was experimentally determined at the indicated concentrations of ACh. Each point corresponds to the mean ± S.D. of at least three patches. The symbols correspond to the following combinations of mutant and wild-type subunits: ■, F = 0, $\alpha_m\beta_{wt}\epsilon_{wt}\delta_{wt}$; ○, F = 2, wild-type; ▲, F = 3, $\alpha_{wt}\beta_{wt}\epsilon_m\delta_{wt}$; ▼, F = 4, $\alpha_{wt}\beta_{wt}\epsilon_m\delta_m$; ♦, F = 4, $\alpha_{wt}\beta_m\epsilon_m\delta_{wt}$ and ●, F = 5, $\alpha_{wt}\beta_m\epsilon_m\delta_m$.

Preserving the aromatic group as in the αF8′Y mutation leads to wild-type kinetics (Fig. 8). However, some recordings of this mutant nAChR revealed some clusters of prolonged openings, accounting for up to 30% of the total clusters. The mean values of P_{open}, mean open duration and closed duration of these clusters for three different recordings were: 0.69 ± 0.02, 2.80 ± 0.30 ms, and 1.19 ± 0.10 ms, respectively. Heterogeneous kinetics have been reported before in wild-type nAChRs (Naranjo and Brehm, 1993) and the number and range of kinetic modes have been shown to increase in mutant nAChRs (Milone et al., 1998; Wang et al., 2000). We thoroughly examined clusters and detected switches from one mode to the other in the same cluster. For example, for one recording containing 272 clusters, 55% of the clusters corresponded to wild-type nAChRs, 31% showed prolonged openings, and 14% showed switches from wild-type to prolonged channels during the course of a single cluster.

All substitutions of βL8′ similarly impair channel gating. As can be seen in Fig. 8, kinetic changes are observed with changes in hydrophobicity, aromaticity, size, or stereochemistry of the side chain. Thus, it seems likely that the β subunit strictly requires leucine to ensure appropriate gating. Replacement of L8′ by other hydrophobic nonaromatic amino acids in the δ subunit does not affect kinetics. Therefore, this subunit seems to be permissive to different hydrophobic amino acids at 8′ but not to hydrophobic aromatic amino acids. After the mutations tested in the ϵ subunit, it seems that this subunit behaves similarly to the δ subunit given that kinetic changes occur in the ϵV8′F although they do not occur in the ϵV8′A.

Discussion

The nAChR is the neurotransmitter-gated ion channel responsible for the rapid propagation of electrical signals at the

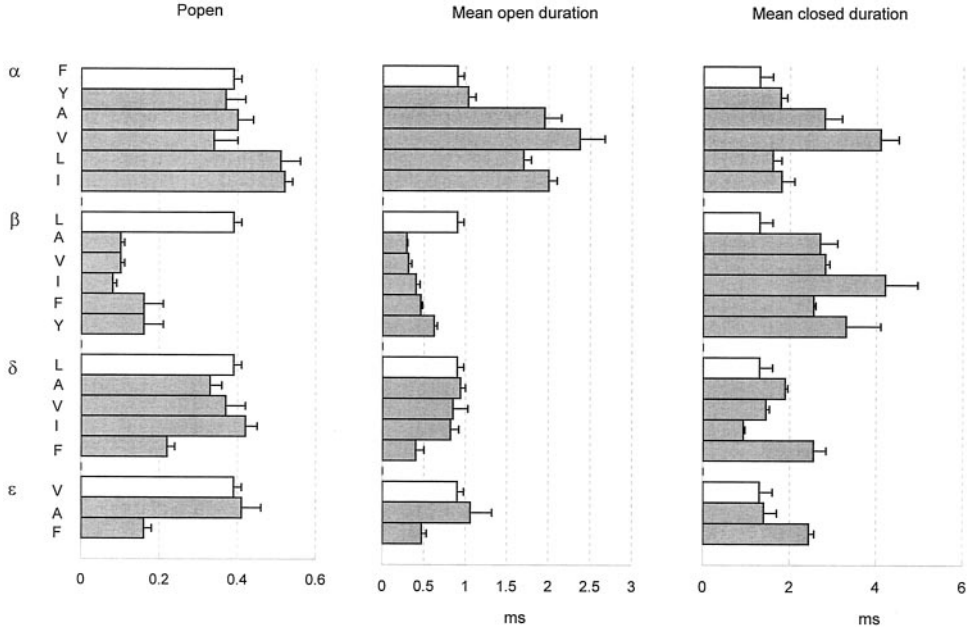

Fig. 8. Mean values of open probability, open channel duration, and closed channel duration of clusters from mutant nAChRs. nAChRs containing a given mutant subunit were activated by 30 μM ACh. For each recording, the distribution of P_{open}, mean open duration and mean closed duration within clusters was plotted. The data correspond to the resulting mean values and SD of at least four different patches for each mutation. Open bars correspond to wild-type subunits.

neuromuscular junction. Although this nAChR is by far the best characterized of the ligand-gated ion channels, the detailed structural mechanisms underlying the rapid depolarization are not yet fully understood. The four transmembrane domains are likely to be involved in the conformational changes associated with gating. According to few lines of experimental evidence showing the contribution of M3 to channel gating [Campos-Caro et al. (1997), Wang et al. (1999), Cruz-Martin et al. (2001)], the present study demonstrates that the M3 segments of all muscle subunits influence both opening and closing steps and reveals the mechanistic and structural bases underlying the contribution to function of position 8′.

Each subunit of the nAChR provides special structural features that, when combined in the whole nAChR, have a functional significance. However, how these specific features were conserved through evolution remains unknown. Position 8′ of the M3 domain is phenylalanine in all heteromeric α subunits, whereas it is a hydrophobic nonaromatic residue in non-α subunits and homomer-forming α subunits. Therefore, the present work shows that this conservation pattern marks residues that contribute to channel gating. However, why the residues were conserved through evolution in such a way remains intriguing given that the structure-function relationships are not conserved among the different subunits.

The present kinetic analysis indicates that mutations at position 8′ of all subunits affect mainly the gating of the nAChR. The diliganded gating equilibrium constant (θ), calculated as β_2/α_2, decreases 13-fold in the F = 5 nAChR with respect to that of wild-type. Such a decrease corresponds to a change in free energy of the gating equilibrium of 1.5 kcal/mol.

A relationship between the number of phenylalanine residues and the duration of the open state is clearly observed (see Fig. 4). Increasing the number of phenylalanine residues at 8′ of M3 leads to progressively larger decreases in the duration of the open state. Although the mutation in the β subunit seems to have a slightly increased effect with respect to mutations at other subunits, the change in the mean open time depends mainly on the final number of phenylalanine residues. Thus, the additive contributions of all subunits to the closing rate indicate that the M3 domains of α, β, δ, and ϵ subunits contribute independently to channel closing through position 8′. Residues at homologous positions in all subunits do not necessarily share a common functional role and, if they do, their functional contributions may or may not be additive. For example, symmetrical and independent contributions to channel gating have been described before for position 9′ of the M2 segment (Filatov and White, 1995; Labarca et al., 1995). Residues at position 12′ of M2 contribute additively but asymmetrically to channel gating (Grosman and Auerbach, 2000). In contrast, some residues in M1 (Wang et al., 1997), M3 (Wang et al., 1999), and M4 (Bouzat et al., 2002) show subunit-specific contributions to channel gating.

The presence of five phenylalanine residues at 8′ of M3 (F = 5) significantly impairs channel opening. After the relationship observed between the number of F residues and the closing rate, we expected that the nAChR lacking F residues at 8′ (F = 0) showed an increased opening rate. However, we were unable to detect such an increase. Because the opening rate constant of wild-type nAChRs (β_2 in Scheme 1) is at the upper limit of reliable estimation, even a modest increase makes this parameter too fast to be resolved (Grosman and Auerbach, 2000). Therefore, we determine the opening rate of F = 0 nAChR channels activated by saturating concentrations of a slowly opening, low-efficacious agonist as choline. At a saturating concentration of choline, the kinetics of the channel can be reduced to that of the closed-to-open reaction (Grosman and Auerbach, 2000; Bouzat et al., 2002). Because the opening rate is slow in the choline-activated nAChRs, this rate constant can be well measured; thus, an increase in such constant can be easily detected. The calculated opening rate constant for F = 0 mutant nAChR is similar to that of wild-type nAChR. Thus, in contrast to what is observed for the closing rate, the opening rate is not affected by reducing the number of phenylalanine residues with respect to that of wild-type nAChRs (F = 2). However, increasing this number from two to five progressively impairs the opening step in the gating pathway.

Mutagenesis studies reveal that the structural bases of the contribution to gating of position 8′ are different for the different subunits. Hydrophobic nonaromatic amino acids replacing αF8′ increase the duration of apparent openings. The β subunit strictly requires leucine at 8′ for appropriate gating: both briefer openings and prolonged intracluster closings are observed either with hydrophobic nonaromatic or aromatic amino acids. In contrast, the δ and ϵ subunits are permissive to different hydrophobic amino acids at 8′ of M3.

The kinetic effects of mutations at 9′ position of M3 have been described in detail by Wang et al. (1999). The gating equilibrium constant decreases 14-fold in nAChRs carrying the mutant αV9′I subunit, about 3-fold in nAChRs carrying βV9′I or ϵA9′V subunits, 1.7-fold in the δV9′I nAChRs, and 60-fold in nAChRs containing the five mutant subunits. Thus, compared with the 13-fold decrease in the gating equilibrium in the F = 5 nAChR here described, position 9′ has more profound effects on gating than position 8′. The structural bases of the functional contributions also differ between positions 8′ and 9′. Mutagenesis studies showed that both volume and stereochemistry at the side chain of residue α9′ contribute to channel gating (Wang et al., 1999). In contrast, at the 8′ position kinetic changes depend on the presence of an aromatic or hydrophobic nonaromatic amino acid in the α, δ, and probably ϵ subunits. However, the relationship between gating and physicochemical properties of the residues at 8′ is complex for the β subunit.

Abnormal activation of nAChR has been shown to underlie congenital myasthenic syndromes (Engel et al., 1998). Moreover, mutation in the residue at a position neighboring the one studied herein has been found to be the cause of the attenuated postsynaptic response observed in the patient (Wang et al., 1999). Consequently, if mutations naturally occurred at the 8′position of M3 of any subunit, they could lead to a congenital myasthenic syndrome, albeit one less severe than the one reported by Wang et al. (1999).

The residues at 8′ of M3 are located on the first third of M3. The pattern of TID labeling of the M3 defines a strip of α-helix in contact with lipids (Blanton and Cohen, 1994). αF284 of *T. californica*, which corresponds to position 8′, has been labeled by TID. In contrast, positions 8′ of β, δ, and γ subunits have not been labeled by TID; they are thus presumably not exposed to the lipids. Assuming that the dispo-

sition of residues in M3 is conserved between mouse and *T. californica*, our results suggest that this position influences gating independently of the packing orientation of the residues with respect to the lipid bilayer. It is therefore possible that the presence of aromatic residues at positions 8′ affects gating by changing their interactions with other residues of the same or other subunits. In conclusion, our results contribute to assigning a functional role to the M3 segment of all muscle nAChR subunits as a component of the channel gating apparatus.

References

Akk G and Auerbach A (1996) Inorganic, monovalent cations compete with agonists for the transmitter binding site of nicotinic acetylcholine receptors. *Biophysical J* **70:**2652–2658.

Baenziger JE and Methot N (1995) Fourier transform infrared and hydrogen/deuterium exchange reveal an exchange-resistant core of alpha-helical peptide hydrogens in the nicotinic acetylcholine receptor. *J Biol Chem* **270:**29129–29137.

Blanton MP and Cohen JB (1994) Identifying the lipid-protein interface of the *Torpedo* nicotinic acetylcholine receptor: secondary structure implications. *Biochemistry* **33:**2859–2872.

Bouzat C, Barrantes FJ, and Sine SM (2000) Nicotinic receptor fourth transmembrane domain. Hydrogen bonding by conserved threonine contributes to channel gating kinetics. *J Gen Physiol* **115:**663–672.

Bouzat C, Bren N, and Sine SM (1994) Structural basis of the different gating kinetics of fetal and adult nicotinic acetylcholine receptors. *Neuron* **13:**1395–1402.

Bouzat C, Gumilar F, Esandi MC, and Sine SM (2002) Subunit-selective contribution to channel gating of the M4 domain of the nicotinic receptor. *Biophys J* **82:**1920–1929.

Bouzat C, Roccamo AM, Garbus I, and Barrantes FJ (1998) Mutations at lipid-exposed residues of the acetylcholine receptor affect its gating kinetics. *Mol Pharmacol* **54:**146–153.

Campos-Caro A, Rovira JC, Vicente-Agulló F, Ballesta JJ, Sala S, Criado M, and Sala F (1997) Role of the putative transmembrane segment M3 in gating of neuronal nicotinic receptors. *Biochemistry* **36:**2709–2715.

Cruz-Martin A, Mercado JL, Rojas LV, McNamee MG, and Lasalde-Dominicci JA (2001) Tryptophan substitutions at lipid-exposed positions of the gamma M3 transmembrane domain increase the macroscopic ionic current response of the *Torpedo californica* nicotinic acetylcholine receptor. *J Membr Biol* **183:**61–70.

Engel AG, Ohno K, Milone M, and Sine M (1998) Congenital myasthenic syndromes. New insights from molecular genetics and patch-clamp studies. *Ann NY Acad Sci* **841:**140–156.

Filatov GN and White MM (1995) The role of conserved leucines in the M2 domain of the acetylcholine receptor in channel gating. *Mol Pharmacol* **48:**379–384.

Grosman C and Auerbach A (2000) Asymmetric and independent contribution of the second transmembrane segment 12′ residues to diliganded gating of acetylcholine receptor channels. *J Gen Physiol* **115:**637–651.

Hamill OP, Marty A, Neher E, Sakmann B, and Sigworth FJ (1981) Improved patch-clamp techniques for high-resolution current recording from cells and cell-free membrane patches. *Pfleug Arch Eur J Physiol* **391:**85–100.

Kyte J and Doolittle R (1982) A simple method for displaying the hydrophatic character of a protein. *J Mol Biol* **157:**105–132.

Labarca C, Nowak MW, Zhang H, Tang L, Deshpande P, and Lester H (1995) Channel gating governed symmetrically by conserved leucine residues in the M2 domain of nicotinic receptors. *Nature (Lond)* **376:**514–516.

Le Novere N and Changeux J-P (1995) Molecular evolution of the nicotinic acetylcholine receptor: an example of multigene family in excitable cells. *J Mol Evol* **40:**155–172.

Liu L-P and Deber CM (1998) Uncoupling hydrophobicity and helicity in transmembrane segments. *J Biol Chem* **273:**23645–23648.

Lugovskoy AA, Maslennikov IV, Utkin YN, Tsetlin VI, Cohen JB, and Arseniev AS (1998) Spatial structure of the M3 transmembrane segment of the nicotinic acetylcholine receptor alpha subunit. *Eur J Biochem* **255:**455–461.

Methot N, Ritchie BD, Blanton MP, and Baenziger JE (2001) Structure of the pore-forming transmembrane domain of a ligand gated ion channel. *J Biol Chem* **276:**23726–23732.

Milone M, Wang HL, Ohno K, Prince R, Fukudome T, Shen XM, Brengman JM, Griggs RC, Sine SM, and Engel AG (1998) Mode switching kinetics produced by a naturally occurring mutation in the cytoplasmic loop of the human acetylcholine receptor epsilon subunit. *Neuron* **20:**575–588.

Naranjo D and Brehm P (1993) Modal shifts in acetylcholine receptor channel gating confer subunit-dependent desensitization. *Science (Wash DC)* **260:**1811–1814.

Ortells MO and Lunt GG (1995) Evolutionary history of the ligand-gated ion-channel superfamily of receptors. *Trends Neurosc* **18:**121–127.

Qin FA, Auerbach A, and Sachs F (1996) Estimating single-channel kinetic parameters from idealized patch clamp data containing missed events. *Biophys J* **70:**264–280.

Sakmann BJ, Patlak J, and Neher E (1980) Single acetylcholine-activated channels show burst-kinetics in the presence of desensitizing concentrations of agonist. *Nature (Lond)* **286:**71–73.

Salamone FN, Zhou M, and Auerbach A (1999) A re-examination of adult mouse nicotinic acetylcholine receptor channel activation kinetics. *J Physiol* **516:**315–330.

Sigworth F and Sine SM (1987) Data transformation for improved display and fitting of single-channel dwell time histograms. *Biophys J* **52:**1047–1052.

Sine SM (1993) Molecular dissection of subunit interfaces in the acetylcholine receptor: identification of residues that determine curare selectivity. *Proc Natl Acad Sci USA* **90:**9436–9440.

Sine SM, Ohno K, Bouzat C, Auerbach A, Milone M, Pruitt JN, and Engel AG (1995) Mutation of the acetylcholine receptor alpha subunit causes a slow-channel myasthenic syndrome by enhancing agonist binding affinity. *Neuron* **15:**229–239.

Unwin N (1993) The nicotinic acetylcholine receptor at 9 Å resolution. *J Membr Biol* **229:**1101–1124.

Unwin N (1995) Acetylcholine receptor channel imaged in the open state. *Nature (Lond)* **373:**37–43.

Wang H-L, Auerbach A, Bren N, Ohno K, Engel AG, and Sine SM (1997) Mutation in the M1 domain of the acetylcholine receptor α subunit decreases the rate of agonist dissociation. *J Gen Physiol* **109:**757–766.

Wang H-L, Milone M, Ohno K, Shen X-M, Tsujino A, Batocchi AP, Tonali P, Brengman J, Engel AG, and Sine SM (1999) Acetylcholine receptor M3 domain: stereochemical and volume contributions to channel gating. *Nature (Lond)* Neurosc. **2:**226–233.

Wang H-L, Ohno K, Milone M, Brengman J, Evoli A, Batocchi A-P, Middleton LT, Christodoulou K, Engel AG, and Sine SM (2000) Fundamental gating mechanism of nicotinic receptor channel revealed by mutation causing a congenital myasthenic syndrome. *J Gen Physiol* **116:**449–460.

Address correspondence to: Dr. Cecilia Bouzat, Instituto de Investigaciones Bioquímicas, Camino La Carrindanga Km 7, B8000FWB Bahía Blanca, Argentina. E-mail: inbouzat@criba.edu.ar